Iraqi J. Laser, Part A, Vol. 2, pp. 21- 27 (2003)

IRAQI JOURNAL OF LASER

Modeling of Plasma Affected Thermal Profile in Solids During Laser Materials Processing

Mohammed A. Hussain (1) **Jewamir M. Saleem** (2) **and Adil A. Alwan** (2)

(1) College of Engineering, Al-Nahrain University, Baghdad, IRAQ
(2) School of Mechanical Engineering, University of Technology, Baghdad, IRAQ

(Received 24 September 2003; accepted 22 November 2003)

Abstract: A new scheme of plasma-mediated thermal coupling has been implemented which yields the temporal distributions of the thermal flux which reaches the metal surface, from which the spatial and temporal temperature profiles can be calculated. The model has shown that the temperature of evaporating surface is determined by the balance between the absorbed power and the rate of energy loss due to evaporation. When the laser power intensity range is 10^7 to10^8 W/cm^2 the temperature of vapor could increase beyond the critical temperature of plasma ignition, i.e. plasma will be ignited above the metal surface. The plasma density has been analyzed at different values of vapor temperature and pressure using Boltzmann's code for calculation of electron distribution function. This analysis has been used to determine the temporal distribution of the net heat flux, which reaches the solid surface. The net heat flux has been proved to vanish at high plasma density. Accordingly the temporal and spatial distributions of temperature profiles within the solid metal have been modeled depending upon the net heat flux which reaches the target surface.

Introduction

The exposure of a solid material to increasing level of laser radiation leads eventually to the formation of plasma at the material surface. As the plasma becomes opaque to the incident radiation, the principal site of energy deposition is shifted from the material surface to the plasma itself.

When a high power intensity laser pulse incident on a metal surface exceeds the air-plasma ignition threshold (10^7 -10^8 W/cm^2), typically 15-20% of the laser-pulse energy appears as residual heat in metal [1]. For highly reflective metals such as aluminum this is several times as much as would be deposited by simple infrared absorption. This phenomenon of plasma-enhanced thermal coupling is clearly attractive for metal heat treatment with increased efficiency.

It has been established by now with the aid of laser sources that the phase transition of a condensed substance into vapor is one of possible mechanisms of disintegration of metals by powerful optical radiation [2]. The absorption of light energy by the metal leads in this case to heating of the target surface layer to a temperature of several thousand degrees. This results in intensive evaporation. The evaporation front (the phase separation boundary) moves into the interior of the target, and this is the case of the disintegration of the target material in the irradiated zone.

Modeling of Laser Induced Plasma Features and Effects

Newstein and Solimene [3] show the extreme sensitivity of the thermal characteristics of the

metal and its vapor to the intensity and duration of the laser field, and the imprecise knowledge of material properties makes the interpretation of experiments difficult in the 10^7-10^8 W/cm^2 range of intensities. In particular, data on metal vapor pressures is sparse in the region of high temperatures attainable under laser irradiation. The enthalpy change as a function of temperature may be estimated by taking the ideal gas form the vapor $[(\frac{5}{3})R_oT_s]$. This gives

$$\Delta H(T_s) = \Delta H(T_b) - \frac{1}{2}R_o(T_s - T_b) \qquad (1)$$

where R_o is the universal gas constant, T_b is the boiling temperature; T_s is metal surface temperature and $\Delta H(T_b)$ is the corresponding latent heat of vaporization; the standard pressure P_o is 1atm. The integrated Clausius-Clapeyron equation is then given by [3] as:

$$P_s(T) = P_o(\frac{T_b}{T_s})^{1/2}\exp\{[\frac{\Delta H(T_b)}{R_oT_b} + \frac{1}{2}][1 - \frac{T_b}{T_s}]\} \qquad (2)$$

where $P_s(T)$ is the vapor pressure at the temperature of metal surface.

The net energy flux incident on the surface is the difference between the flux of laser radiation and the flux of energy carried off by the ablated mass. Applying steady-state conservation laws for matter and momentum, flux at the metal/vapor interface [4], It has been found that the pressure in the vapor adjacent to the metal surface is decreased from the saturation vapor pressure by the factor 1 / (1+γ), where γ is the specific heat ratio, considered here as having the value of 5/3, and defined as c_v/c_p where c_p and c_v are the specific heat at constant pressure and at constant volume respectively. Newstein and Solimene [3] take the velocity of the vapor to be the speed of sound at the surface temperature of the metal. Then the net flux of energy incident on the metal surface is

$$Q_{netflux} = (1-R)I_o - 0.82(\frac{P_s\Delta H}{R_oT_s(1+\gamma)} + \frac{v^2}{2}) \qquad (3)$$

where R is the metal reflectivity and I_o is the intensity of the incident laser radiation.

The factor of (0.82) was derived by Anisimov [5] to account for the fraction of the emitted flux, which does not re-condense. v is the velocity of vapor which is equal the speed of sound at the initial stage of vapor (at boiling temperature).This is means that about 18% of the energy used for evaporation will be restored by the metal surface.

These analyses suggest that target heating occurs principally by the absorption of thermal emission from the laser-heated plasma. The temperature of the plasma is around 2 x 10^4 ^{o}C. This is consistent with theoretical results obtained by Ref. [6], the peak of blackbody thermal emission lies in the near ultraviolet, where metals have much higher absorptance than in the infrared; consequently this can be an efficient thermal-coupling process.

Mathematical Model

Newstein and Solimene [3] discussed one-dimensional form of the thermal diffusion equation

$$\frac{\partial H}{\partial t} = \frac{k}{\rho}\frac{\partial^2 T}{\partial x^2} \qquad (4)$$

which expresses the fact that the time rate of change of the specific enthalpy ($\partial H / \partial t$) equals the divergence of the thermal flux. The temperature change is related to the enthalpy change by the specific heat.

The boundary condition for the thermal diffusion equation is that, at x = 0 (the surface where the light is absorbed), the thermal flux $(-\frac{k}{\rho}\frac{\partial T}{\partial x})$ equals the net absorbed flux. This condition is implicitly dependent on temperature because the flux of energy associated with the ablated material is temperature dependent.

Since the enthalpy H = c T [7], where c is the specific heat of metal, then equation (4) becomes

$$\frac{\partial cT}{\partial t} = \frac{k}{\rho}\frac{\partial^2 T}{\partial x^2} \qquad (5)$$

$$c\frac{\partial T}{\partial t} = \frac{k}{\rho}\frac{\partial^2 T}{\partial x^2} \qquad (6)$$

where $\alpha = \frac{k}{\rho c}$, thus equation (6) becomes

$$\frac{1}{\alpha}\frac{\partial T}{\partial t}=\frac{\partial^2 T}{\partial x^2} \tag{7}$$

The new scheme used to calculate the temperature of vapor and plasma above metal surface depends upon these assumptions, which were reported by Ref. [3], and include the term $Q_{netflux}$ for surface heat sources taken to solve the nonlinear differential equations for different positions of x ,y and z coordinates:

$$Q_{surf.}=\frac{Q_{netflux}}{\delta}\exp((-\frac{\sqrt{x^2+y^2+z^2}}{\delta})(\frac{x^2+y^2}{\omega^2})) \tag{8}$$

where δ is absorption coefficient, and ω is the laser spot radius.

The new scheme is represented in Cartesian coordinates to illustrate the temperature distribution upon the surface of metal.

Cartesian Coordinates Analysis:

The form of equation (7) in three-dimensional Cartesian coordinates (for the coordinate system shown in the sketch below) is written as:

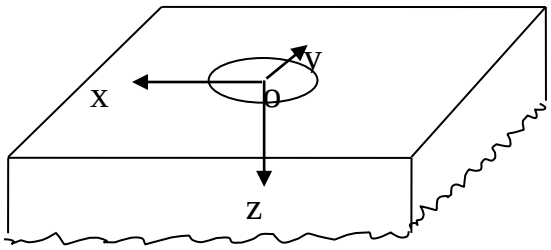

$$\frac{1}{\alpha}\frac{\partial T}{\partial t}=\frac{\partial^2 \mathrm{T}}{\partial \mathrm{X}^2}+\frac{\partial^2 \mathrm{T}}{\partial \mathrm{Y}^2}+\frac{\partial^2 \mathrm{T}}{\partial \mathrm{Z}^2}+\frac{Q}{k} \tag{9}$$

where k is the metal thermal conductivity.

Three-dimensional Cartesian model has been developed to give another solution to the temperature distribution of metal as a function of vapor and plasma temperature initiation above the surface metal. The representation of equation (9) in explicit technique form is:

$$T_{i,j,k}^{n+1}=\lambda T_{i+1,j,k}^{n}+(1-6\lambda)T_{i,j,k}^{n}+\lambda T_{i-1,j,k}^{n}+\lambda T_{i,j+1,k}^{n}+\lambda T_{i,j-1,k}^{n}+\lambda T_{i,j,k+1}^{n}+\lambda T_{i,j,k-1}^{n}+\frac{Q(i,j,k)}{k}\alpha\Delta t \tag{10}$$

where $\frac{\alpha\Delta t}{\Delta x^2}=\frac{\alpha\Delta t}{\Delta y^2}=\frac{\alpha\Delta t}{\Delta z^2}=\lambda$,

and $\Delta x=\Delta y=\Delta z$. In the new scheme another assumption is made for z = 0 (the surface where the light is absorbed):

$$Q_{netflux}=-\frac{k}{\rho}\frac{\partial T}{\partial z} \tag{11}$$

The boundary condition of equation (11) is represented in finite difference form as:

$$Q_{netflux=}=-\frac{k}{\rho}\frac{T_{i,j,k+1}^{n}-T_{i,j,k-1}^{n}}{2\Delta z} \tag{12}$$

and the initial condition is $T(x,y,z,0)=T_o$, then substituting the boundary condition described by equation (12) in equation (10), yields:

$$T_{i,j,k}^{n+1}=\lambda T_{i+1,j,k}^{n}+(1-6\lambda)T_{i,j,k}^{n}+\lambda T_{i-1,j,k}^{n}+2\lambda T_{i,j+1,k}^{n}+2\lambda T_{i,j,k+1}^{n}+\frac{\alpha\Delta t}{\Delta x}\frac{\rho 2Q_{netflux}}{k}+\frac{Q(i,j,k)}{k}\alpha\Delta t \tag{13}$$

A numerical solution of above equation that depends upon the explici‧ technique to calculate the surface temperature has been implemented in a compu‧er program. This will present more details for predicting temperature distribution in the x, y and z axes depending upon the boundary conditions and the net flux of energy which is absorbed by the metal. The surface temperature is a function of the vapor and plasma initiation above the surface.

Calculation of Plasma and Vapor Density

It has been considered that the evaporation of metals at light fluxes corresponding to target surface temperature T_s is lower than the critical temperature T_c. This analysis is based to a considerable degree on certain already known results concerning the kinetics of evaporation and establishment of hydrodynamic motion of vapor from an evaporating target.

Feeding back the value of temperature results from the model in equation (2), a wide range of vapor pressure as a function of surface temperature can be established.

Smith [4] showed that the vapor is regarded as an ideal gas, and absorption of light in it is neglected, then the initial vapor velocity is equal to the local sound velocity. This is called the critical state as $v = u^*$. Where u^* is the speed of sound. Patrick and Oosthuizen [8] showed an ideal gas flow at Mach number $M' = 1$ and the flow is sonic, where $M' = v / u^*$. Then the velocity v is determined by an obvious formula that follows from energy considerations

$$v = u^* = \sqrt{\gamma R_o T_s} \tag{14}$$

where the velocity of vapor is calculated as a function of temperature.

Anisimov [5] showed the computation of the flow J_c of atoms condensed back on the surface of the metal amounts to approximately 18% of the flow J_* of the vaporized atoms depending upon the Boltzmann equation, where

$$J_* = nes\sqrt{K_b T_s / 2\pi m} \tag{15}$$

$$J_c = 0.18 J_* \tag{16}$$

where nes is the electron density, K_b is the Boltzmann constant, and m is the mass flow rate of vapor. The mass flow rate can be calculated as [9] :

$$m = \frac{(1-R)I_o}{L_v} \tag{17}$$

where L_v is the specific latent heat of vaporization. Therefore the kinetics of vapor condensation must be taken into account in computation of flow in rarefaction wave. Boltzmann equation is necessary for the calculation of flow parameters at the acoustic point.

Weyl et al. [9] reports on equation depending upon Boltzmann code of calculation of electron distribution function to calculate the electron density as:

$$nes = 2.8x10^9 (I_{inc})^{0.48} (T_s)^{0.49} P_s \tag{18}$$

where I_{inc} is the incident laser power intensity. With feeding the surface temperature which results from the model after critical temperature of metal to calculate different values of electron density at different values of pressure (which is function of surface temperature). At this point it has been shown that the net heat flux starting to decrease as the flow J_c increases (as plasma ignition). This shows how the plasma plume prevents the heat flux from being absorbed by the metal surface and the re-radiation starts.

These analyses give a good description of plasma mechanism by using the new scheme here which appears to be reliable for the calculation of the surface thermal transient.

Results and Discussion

In the analysis of the metal heating stage, a method of extrapolating existing data of $\Delta H(T_s)$ and $P_s(T)$ on material properties into the temperature range of interest has been presented. Because of the sensitive nature of the dependence of vapor pressure on temperature, the results based on the extrapolated values differ significantly from those obtained using a more approximate expression [10]. A numerical solution of the nonlinear heat transfer equation has led to surface temperature values substantially different from the predications of the steady-state model of surface evaporation presented by Newstein and Solimene [3].

A 3-dimensional Cartesian model gives another prediction of spatial and temporal temperature distribution below and above the critical temperature of the two metals used. How these temperature results which present the mechanism of vapor and plasma initiated above the surface metals has been shown. These results depend upon the amount of heat flux, which is absorbed by vapor and the amount condensed back through the mechanism of plasma formation. These results are illustrated in figures (1) to (4) for aluminum and stainless steel.

Figures (5) and (6) illustrate the spatial temperature distribution in aluminum and stainless steel with depth (z) at different time intervals and at power intensity 10^7 W/cm^2 when plasma is initiated above the metal surface.

The prompt initiation of the plasma above metal surfaces irradiated by a CO_2 laser pulse in an intensity range of 10^7–10^8 W/cm^2 is modeled by the use of Boltzmann code. The

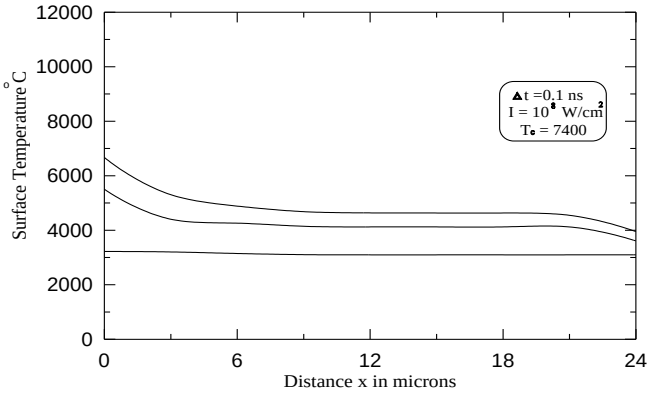

Figure (1) spatial temperature distribution in aluminum for different heating time when vapor started above the surface.

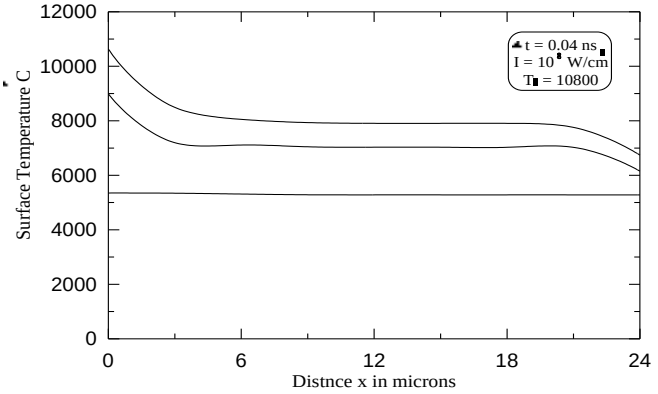

Figure(2) spatial temperature distribution in stainless steel for different heating time when vapor started above the surface.

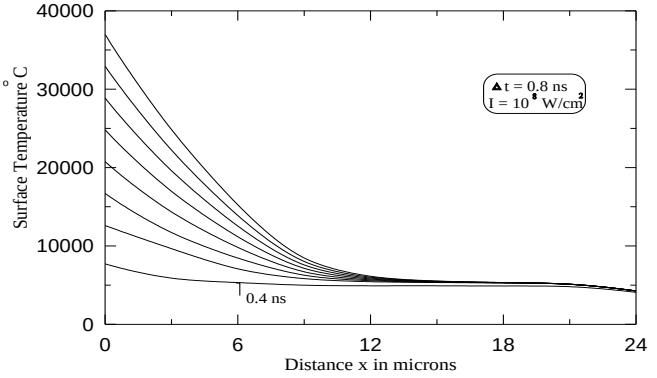

Figure (3) spatial temperature distribution in aluminum for different heating times when plasma initiated above the surface.

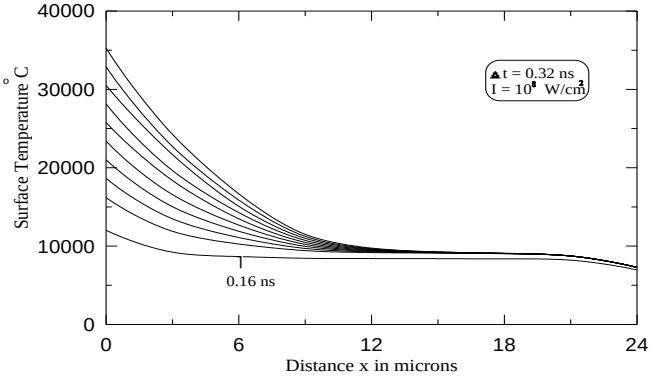

Figure (4) spatial temperature distribution in stainless steel for different heating times when the plasma initiated above the surface.

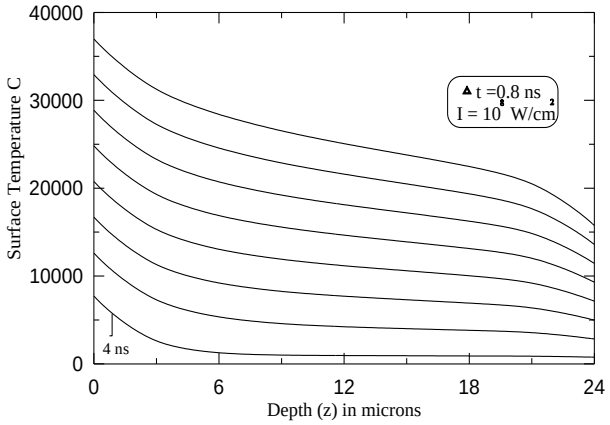

Figure (5) temperature profile against metal depth for different heating times in aluminum when plasma initiated above the surface.

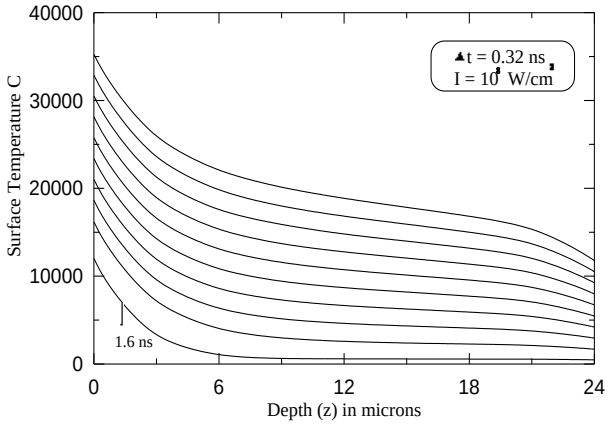

Figure (6) temperature profile against metal depth for different heating times in stainless steel when plasma initiated above the surface.

166

initiation mechanism is assumed to be the vaporization of flakes or surface defects that are thermally insulated from the bulk surface, followed by laser-induced break-down in the vapor.

It has been found that using Boltzmann code the delay time for populating the first excite impact ionization of this state leads to a very short avalanche break-down.

Figures (7) and (8) show the plasma density and the net heat flux for aluminum at a power intensity of 10^8 W/cm^2. Similar behavior has been experienced with stainless steel as shown in figures (9) and (10). Effective plasma density starts at the critical temperature of metal. The critical temperature of aluminum is 7400^{o}C and for stainless steel is about 10800^{o}C [11]. Plasma density increases with time after this point.

The net heat flux, which is absorbed by the target metal, decreases with time when plasma is

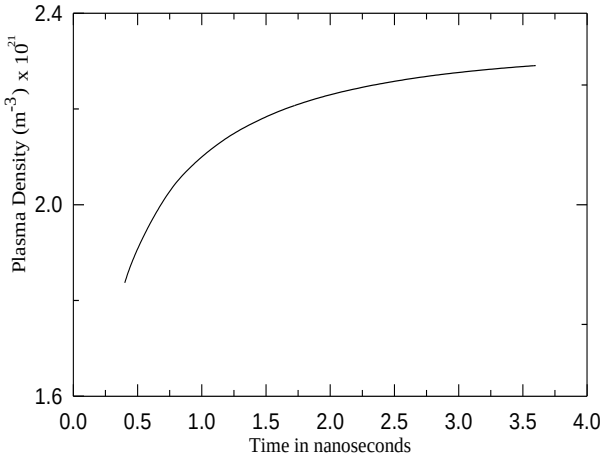

Figure (7) plasma density as a function of time initiated above the surface of aluminum at I = 10^8 W/cm^2.

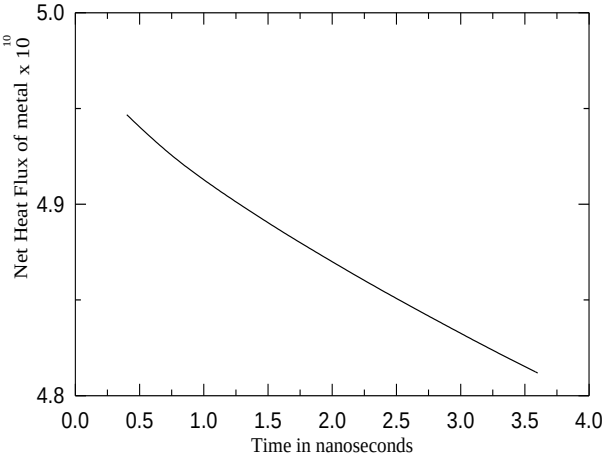

Figure (8) net heat flux of metal as a function of time in aluminum at I = 10^8 W/cm^2.

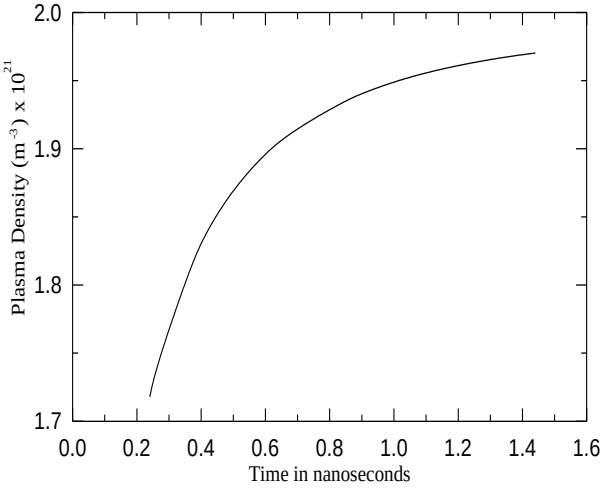

Figure (9) plasma density as a function of time initiated above the surface of stainless steel at I = 10^8 W/cm^2.

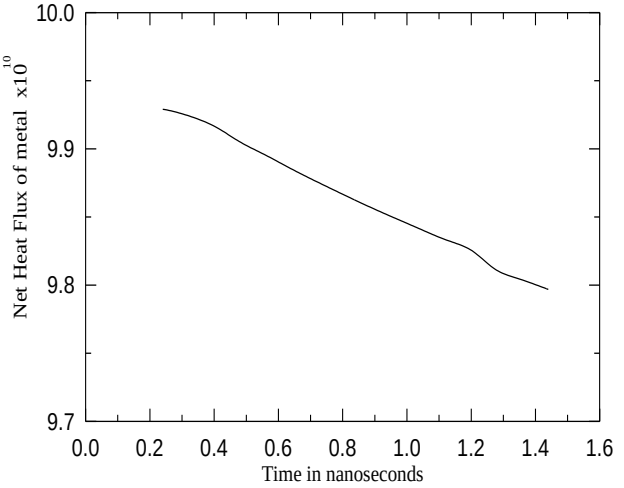

Figure (10) net heat flux of metal as a function of time in stainless steel at I = 10^8 W/cm^2.

initiated. Thus plasma makes a plume to prevent the laser radiation to be absorbed by the metal surface. Then the reradiation starts.

These figures present a new suggestion of plasma mechanism formation and how the net heat flux that reaches the metal surface diminishes at high values of plasma density. This is consistent with experimental results obtained by Al-Ugaili [12]. This reference presented experimental studies of optical breakdown on metal surfaces irradiated by high power laser pulses, and the proportion of energy absorbed (and reflected) by the plasma. Al-Ugaili has proved that the metal surface is entirely shielded from receiving any laser flux due to the formation of high density plasma over its surface.

Conclusions

Plasma initiation above metallic surfaces irradiated with laser fluxes of 10^7- 10^8 W/cm^2 is simulated. It has been concluded that:

a) Simulation of plasma has led to estimating the net heat flux, which reaches the material surface. It has been found the net heat flux is badly attenuated at a high of plasma density.
b) Modeling the temperature profile within the material would determine the type of process, which might be performed.
c) The results can be used to estimate the optimum pulse duration, to prevent energy loss due to plasma formation during material processing.
d) Estimation of the effective energy received

from long laser pulses by the material surface, and that is from calculating the down time caused by plasma shielding.

References

[1] J. A Makay, and F. Schriemp, *Transient Surface Heating of Metals by CO_2 Laser Pulses with Air-Plasma Ignition*, J. Appl. Phys. **50**, 5202- 5 (1979).

[2] V. A. Batanov, F. V. Bunkin, A. M. Prokhorov and V.B. Fedokov, *Evaporation of Metallic Targets Caused by Intense Optical Radiation*, J. Sov. Phys. JETP **36**, 311- 22 (1973).

[3] M. Newstein, and N. Solimene, *Laser Metal Interaction in Vacuum*, IEEE J. of Quantum Electronics **QE-17**, 2085-91 (1981).

[4] D. C. Smith, *Gas Breakdown Initiated by Laser Radiation Interaction with Aerosols and Solid Surfaces*, J. Appl. Phys. **48**, 2217- 25 (1977).

[5] S. I. Anisimov, *Vaporization of Metal Absorbing Laser Radiation*, J. Sov. Phys. JETP **27**, 182- 3 (1968).

[6] J. A. McKay and J. T. Schriempe, *Pulsed CO_2 Lasers for the Surface Heating and Melting of Metal*s, IEEE J. of Quantum Electronics **QE-17**, 2008- 15 (1981).

[7] L. N. Gutman, *On the Problem of Heat Transfer in a Phase-Change Slab Initially Not at the Critical Temperature*, J. Heat Transfer **109**, 5- 9 (1987).

[8] P. Patrick and H. Oosthuizen "Compressible Fluid Flow," McGraw-Hill, N.Y. 1997.

[9] G. Weyl, A. Pirri, and R. Roo, *Laser Ignition of Plasma of Aluminum Surface*, AIAA Journal **19**, 460- 69 (1981).

[10] J. A. McKay. and J. T. Schrie, *Anomalous IR Absorption of Aluminum under Pulsed 10.6μm Laser Irradiation in Vacuum*, J. Appl. Phys. Lett. **359**, 433- 34 (1979).

[11] R. C. Weast, "Hand Book of Chemistry and Physics" CRC Press, Florida, 1987-1988.

[12] E. A. K. Al-Ugaili, *Optical Breakdown and Energy Absorption of Laser Produced Plasma on Metallic Surfaces*, M.Sc Thesis, Saddam University, 2001.

نمذجة السلوك الحراري المتأثر بالبلازما في المواد الصلبة خلال معالجتها بالليزر

محمد عبد الامير حسين [1] **جوامير مجيد سليم** [2] **عادل عباس علوان**[2]

(1) كلية الهندسة / جامعة النهرين ، بغداد ، العراق

(2) قسم الهندسة الميكانيكية / الجامعة التكنولوجية ، بغداد ، العراق

الخلاصة

يستعرض هذا البحث طريقة جديدة للتعشيق الحراري بوجود طور البلازما حيث تم احتساب التوزيع الزمني للفيض الحراري الواصل الى سطح المعدن ثم احتساب التوزيع الحراري المكاني والزمني في المعدن . يبين هذا النموذج بان درجة حرارة السطح المتبخر تعتمد على الفرق بين القدرة الممتصة وبين المعدل الزمني للطاقة المستهلكة في التبخر ، فعندما تكون شدة قدرة الليزر الساقطة بين 10^7 و 10^8 واط/سم^2 سترتفع درجة حرارة البخار وتتعدى الدرجة الحرجة لقدح البلازما ، وبذلك ستتكون البلازما على سطح المعدن . تم احتساب كثافة البلازما عند قيم مختلفة لضغط ودرجة حرارة البخار على سطح المعدن وذلك باستخدام علاقة بولتزمان الخاصة بحساب دالة التوزيع الالكتروني . وقد استخدم هذا الاحتساب في تحليل التوزيع الزمني لصافي الفيض الحراري الذي سيسقط على سطح المعدن الصلب . لقد اثبت هذا التحليل النظري ان صافي الفيض يتلاشى عندما تكون كثافة البلازما عالية . وهكذا فقد تم نمذجة التوزيع المكاني والزمني للسلوك الحراري في المعدن الصلب بالاعتماد على صافي الفيض الحراري الواصل لسطح المعدن .